

Mössbauer-Effect Measurements in Antiferromagnetic FeCl_3 [†]

J. P. Stampfel,* W. T. Oosterhuis, and B. Window‡

Physics Department, Carnegie-Mellon University, Pittsburgh, Pennsylvania 15213

F. deS. Barros

Instituto de Física da Universidade, Federal do Rio de Janeiro, Brazil

(Received 29 June 1973)

Mössbauer-effect data for single-crystal specimens of anhydrous ferric chloride are presented which cover the region in the H - T plane for H less than kOe and the temperatures less than 300 K. The magnetic phase boundaries between the paramagnetic, antiferromagnetic, and "spin-flop" phases are observed. The zero-field data show antiferromagnetic order with $T_N = 8.76$ K, and the hyperfine field is found to obey a power law of the form $H_{\text{hf}}(T) = H(0) B(1 - T/T_N)^\beta$, where $\beta = 0.156$, $B = 1.035$, and $H(0) = 495$ kOe. This power law holds for the full range of temperatures less than T_N . The data just below T_N show extreme broadening in the Mössbauer spectrum, reminiscent of relaxation effects in paramagnets, most likely due to critical slowing down. The data in zero field are consistent with the unusual spiral-spin structure found by neutron diffraction. However, for fields larger than 15 kOe applied in the c direction, the Mössbauer data show two distinct hyperfine fields as if there were two sublattices instead of a spiral structure. When the applied field in the crystalline c direction exceeds 40 kOe (at $T = 4.2$ K), a spin reorientation takes place similar to what one finds in a "spin flop." The field necessary to "flop" these spins increases with temperature to about 48 kOe at 8.4 K where a triple point exists, and the Néel temperature decreases with increasing applied field. The data in applied fields also show the extreme broadening of the resonance lines as the critical temperature is approached. The data in the paramagnetic region show the influence of the magnetic interactions. The results suggest that FeCl_3 is possibly near a tricritical point.

I. INTRODUCTION

Anhydrous FeCl_3 crystallizes in a hexagonal layer structure isomorphic with BiI_3 and the low-temperature phase of CrCl_3 . X-ray structure classifications were made first by Wooster¹ and later by other investigators,² who assigned it to the rhombohedral space group $R\bar{3}$ with parameters $a = 6.76$ Å and $\alpha = 53^\circ 11'$ for the bimolecular unit cell. The hexagonal cell containing six formula units has parameters $a = 6.06$ Å and $c = 17.43$ Å. The structure is a hexagonal close pack of chlorines with the irons filling two-thirds of the octahedral interstices between every other pair of Cl layers perpendicular to the c direction. The iron ions form a honeycomb arrangement in these layers (Fig. 1). Each iron ion is at the center of a nearly perfect octahedron of chlorines. Because of the layer-type structure in FeCl_3 and the distance between the iron ions in the c direction, one expects very different magnetic interactions in the plane as compared to the c direction. Several investigations³ have been undertaken recently to examine the critical-point properties of such materials with anisotropic exchange. We have made a similar effort in the case of FeCl_3 using nuclear gamma resonance (NGR)—the Mössbauer Effect.

The first magnetic measurements on FeCl_3 below room temperature were made by Starr,⁴ who reported the magnetic susceptibility in fields to 32 kOe at temperatures down to 13.9 K. No mag-

netic ordering was observed, but a deviation from Curie-Weiss behavior was noted at low temperatures. A paramagnetic Néel temperature of 11.5 K was found, suggesting antiferromagnetism with a Curie constant of 4.07 emu/mole.

Cable *et al.*,⁵ using neutron diffraction, indicated the magnetic structure to be antiferromagnetic with a Néel temperature of 15 ± 2 K. This transition temperature was supported by NGR data taken by Kocher⁶ and magnetic hyperfine structure as seen in the work of Pfletschinger.⁷ The complicated magnetic structure deduced by Cable *et al.* consists of antiferromagnetic ordering of near-neighbor iron ions in the c direction and superimposed on this a proper helical structure propagating along the $[14\bar{5}0]$ direction with turn angle $2\pi/15$ in successive $(14\bar{5}0)$ planes [the spins lie in $(14\bar{5}0)$ planes]; see Fig. 1. In that work, coherent magnetic scattering was reported at temperatures as high as 43 K. An ordered-moment characteristic of high-spin ferric ions ($5.92\mu_B$) was not found even at temperatures where the sublattice magnetization should have been saturated. Another interesting feature was the presence of an antiferromagnetic domain structure. Three domains were found (corresponding to the threefold symmetry about the c axis) and transformations into a single-domain structure could be effected with fields as low as 8 kOe applied perpendicular to c .

Susceptibility measurements were extended down to 4.2 K by Jones and co-workers⁸ who found a

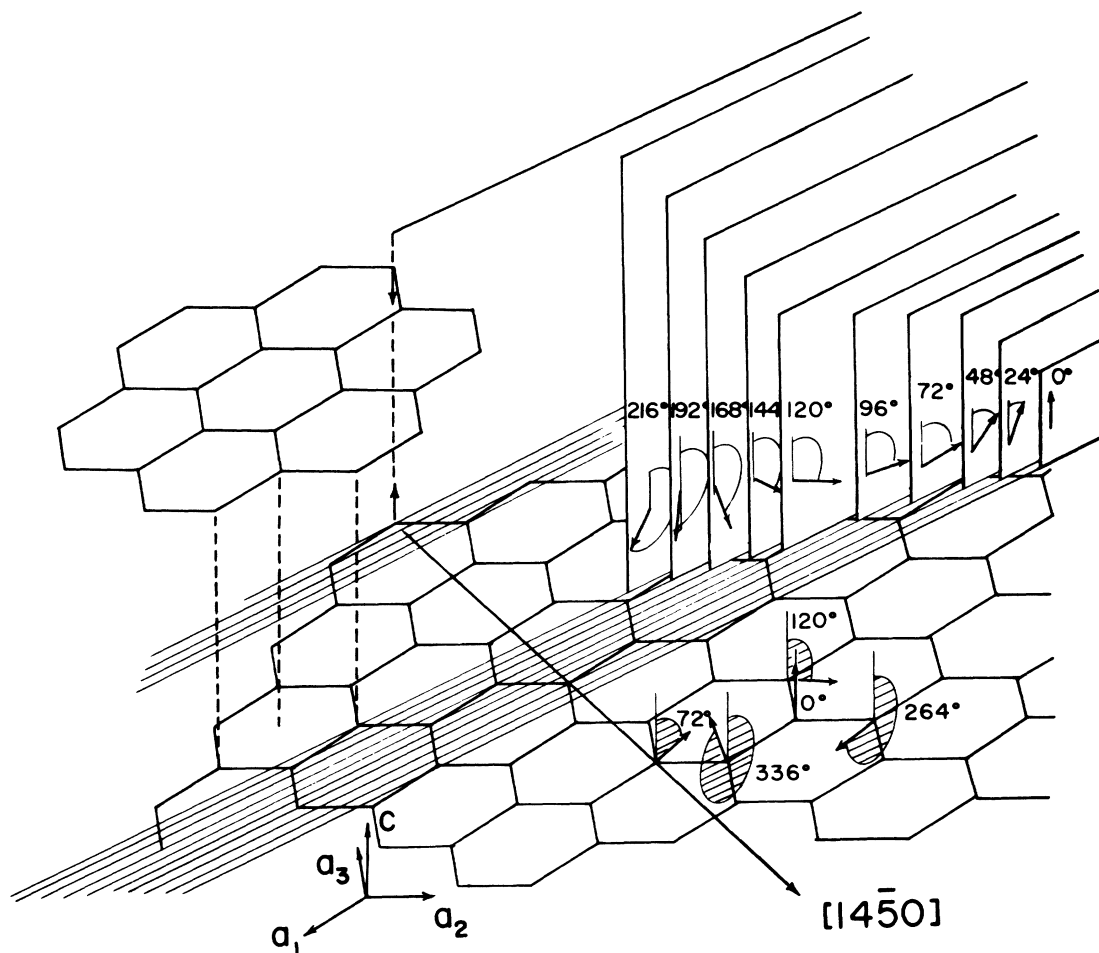


FIG. 1. Diagram showing the zero-field spin configuration in FeCl_3 . The iron ions occupy $\frac{2}{3}$ of the interstices of a hexagonal-close-packed structure of chlorine ions. The iron ions are at the vertices of the honeycomb lattice which lies in the plane perpendicular to the c axis. There is antiferromagnetic coupling in the c direction, whereas the spins in the plane are in a spiral whose axis is in the $[14\bar{5}0]$ direction. The rotation of spins in the $(14\bar{5}0)$ planes are indicated in degrees of angle in the upper right section. The orientation of near-neighbor spins is indicated in the lower right section.

Néel temperature of 9.75 ± 0.2 K and a paramagnetic Néel temperature $\Theta = 30.5$ K for the data below 77 K. Bizette⁹ measured the magnetization of a single crystal in the range 4.2 to 30 K in fields up to 23 kOe and found $\Theta = 14$ K. Anomalies in the reciprocal susceptibility occur near 25 and about 9 K.

The complicated magnetic structure proposed for FeCl_3 is not well understood theoretically. The spiral in FeCl_3 differs from the helical ordering in the heavy rare earths in two distinct ways. First, the spiral axis is not along the c axis, as is common in many rare-earth cases, and second, the moments in the planes normal to the spiral axis are antiferromagnetically aligned in FeCl_3 compared with the ferromagnetic alignment in the rare earths. A spiral structure reminiscent of

that in FeCl_3 was found by Cable and co-workers for MnI_2 ¹⁰ and attempts by Nagamiya and Moriya¹¹ to understand that structure were not fully successful. Their results showed that the basal-plane components of the spiral axis depended almost entirely on the in-plane exchange interactions but over-all a delicate balance of exchange, anisotropy, and dipolar interaction energies were required by the model.

II. EXPERIMENTAL

Single-crystal specimens were prepared by two different techniques. Some early experiments were done on crystals grown by sublimation as described by Schafer.¹² In this case the starting ferric chloride was prepared by reacting carbonyl iron in a chlorine-gas stream. The powder thus

manufactured was sealed in an evacuated Pyrex ampoule. The ampoule was suspended first in a benzophenone boiling bath ($T=304^\circ\text{C}$), then in a phthalic acid anhydride–10% anthraquinone boiling bath ($T=285^\circ\text{C}$). In this final stage the material sublimed forming platelets on the cooler upper walls of the ampoule. Competition between neighboring outgrowths prevented the formation of large-area plates and twinning was common.

Most of the experiments described in this paper were done with samples cleaved from large boules grown by a Bridgman-furnace method suggested for materials of the BiI_3 structure by Bené.¹³ Here the starting material was commercial anhydrous FeCl_3 powder (Fisher Scientific). The powder was placed in a Pyrex-glass ampoule sealed under vacuum and the ampoule suspended in a Bridgman furnace. The top of the furnace was maintained at a constant temperature of approximately 315°C by a controller and the bottom furnace was heated to about 180°C by an autotransformer. The temperature gradient at the freezing plane (the melting temperature of anhydrous ferric chloride is 306°C ¹⁴) was approximately $20^\circ\text{C}/\text{cm}$. After the material had become molten in the top furnace it was lowered by a gear train and synchronous motor at a rate of 1 cm/day. Boules as large as 18 mm in diameter and 30 mm in length were grown in this way. These crystals gave no evidence of other iron-containing chemical phases as had been found in the vapor-grown crystals.

The high chemical activity and deliquescence of ferric chloride create serious storage and handling problems. FeCl_3 reacts with oxygen to form FeOCl . For this reason it was handled in a glove box with a dry-nitrogen atmosphere and a layer of Drierite desiccant on its bottom, or handled under liquid nitrogen. FeCl_3 is so hygroscopic that a sample exposed to air becomes a puddle of liquid within a matter of minutes. Ferric chloride was found to hydrolyze silicone vacuum grease, which is often used to protect materials or bond them for low-temperature work. It did not react with, but took water from, commercial *n*-decane and cyclohexane, even after they had been dried with sodium metal. Reactions also occurred with petroleum jelly and commercial mineral oil (Nujol). The final solution was to coat the inside of sample holders with paraffin wax, insert the crystal, and cover it with Parafilm and squeeze this down with the sample-holder cover plate. These samples were then stored and handled under liquid nitrogen. No reaction was ever found between the paraffin and FeCl_3 and the samples showed no decomposition.

The transmission samples were cleaved from the boules in a glove box. Ferric chloride has a layer structure and cleaves normal to the *c* axis.

Attempts to cut the boules in other directions using a razor blade caused the layers to separate. This made it impossible to prepare any but basal-plane plates even though bulk crystals were available. The softness of the ferric chloride and the encumbrance of the glove box made it difficult to control the thickness of the plates and optimum sample thickness could not be achieved. Typical thickness was $65\ \mu\text{m}$; optimum thickness $25\ \mu\text{m}$.

The single crystals of FeCl_3 survived many temperature cycles in going below the transition temperature and back.

Mössbauer spectra were taken in transmission geometry utilizing a constant-acceleration spectrometer with a multichannel analyzer operated in the time mode. The spectrometer was calibrated at regular intervals using an iron foil whose spectra were compared to the values of Violet and Pipkorn.¹⁵ The sources of ^{57}Co in palladium foils were maintained at room temperature and gave a linewidth (full width at half-maximum—FWHM) of $0.22 \pm 0.003\ \text{mm}/\text{sec}$ for a thin iron absorber.

A superconducting magnet (Oxford Instruments) provided fields up to 60 kOe. Most spectra were taken with the field parallel to the γ beam, with a few in the perpendicular geometry. The data at and below 4.2 K were taken with the sample immersed in the refrigerant. Temperatures below 4.2 K were achieved by pumping on the liquid-helium bath and the pressure was controlled by a Cartesian diver manostat. The data above 4.2 K were taken with the sample imbedded in a copper block with aluminum-foil windows. The block was suspended in a vacuum by a phenolic board and surrounded by a shield at 4.2 K. The temperature of the copper block was maintained by a manganin heater which was regulated by an electrothermal feedback system.¹⁶ The temperature was monitored by an Allen-Bradley 100- Ω carbon resistance thermometer and also by an Au(3-at. % Fe)—chromel-*P* thermocouple. Each thermometer was embedded in the copper block. The temperature was monitored on a chart recorder and showed variations of less than 0.040 K during the course of each experiment.

III. EXPERIMENTAL RESULTS AND ANALYSIS

A. Paramagnetic Region (*P*)

At temperatures greater than the Néel temperature the data behave as expected for a paramagnet. In the absence of an applied field there is only a single resonance, whereas a hyperfine field is induced by the presence of an applied field H_0 (Fig. 2). The nuclear Hamiltonian which describes this behavior is

$$\mathcal{H}_N = \vec{I} \cdot \vec{A} \cdot \overline{\langle \vec{S} \rangle}_T - g_N \mu_N \vec{H}_0 \cdot \vec{I}, \quad (1)$$

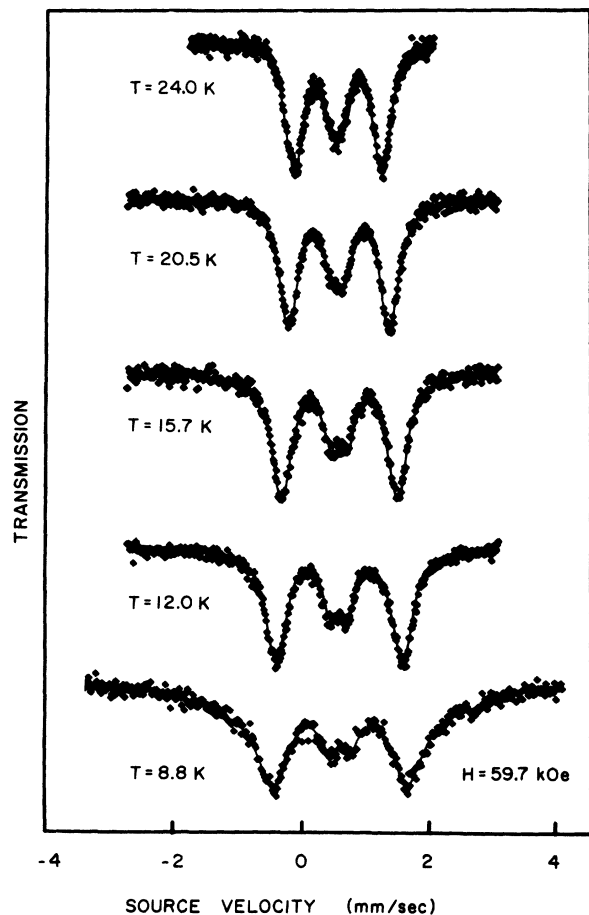


FIG. 2. Mössbauer spectra for single crystals of FeCl_3 with a field of 59.7 kOe applied in the c direction parallel to the gamma beam. The temperature is varied over the paramagnetic region and the variation in the hyperfine field can be seen.

where

$$\langle \vec{S} \rangle_T = \frac{\sum_j \langle j | \vec{S} | j \rangle e^{-E_j/kT}}{\sum_j e^{-E_j/kT}} \quad (2)$$

and the electronic states $|j\rangle$ are linear combinations of the spin states $|\pm \frac{5}{2}\rangle$, $|\pm \frac{3}{2}\rangle$, $|\pm \frac{1}{2}\rangle$. The electronic Hamiltonian for the paramagnetic 6S state with axial symmetry is

$$\mathcal{H}_e = DS_z^2 + 2\mu_B \vec{H}_0 \cdot \vec{S}. \quad (3)$$

As the temperature is lowered, the more energetic states of the spin sextet are depopulated and the thermal expectation value of the spin sensed by the nuclear moment rises toward its saturation value.

The applied field helps to spread these states $|j\rangle$ in energy and thus increases the depopulation of the excited states for a given temperature. The greater is the ratio H_0/T , the greater the induced hyperfine field.

The field is applied along the c direction in the single crystal, which we take as the z axis in Eqs. (1)–(3).

The internal field is related to the thermal expectation value $\langle S \rangle_T$ as $H(T) = A \langle S \rangle_T / g_N \mu_N$. We take $H(0) = A \langle \frac{5}{2} \rangle / g_N \mu_N = 495$ kOe as the value extrapolated to $T=0$ from the data in the ordered region. In the case where $D=0$, the temperature dependence of the internal field is given by the Brillouin function $H(T)/H(0) = B_{5/2}(H_0/T)$. However, the data for FeCl_3 in the paramagnetic region show that the hyperfine field dependence on H_0 and T does not agree with the simple Brillouin function $B_{5/2}(H_0/T)$. (See Fig. 3).

The disagreement between the hyperfine field expected from Eq. (3) and experiment is a manifestation of exchange interactions above the critical temperature of 8.76 K. If this is so then we could use a molecular field Hamiltonian for a two-sublattice antiferromagnet,

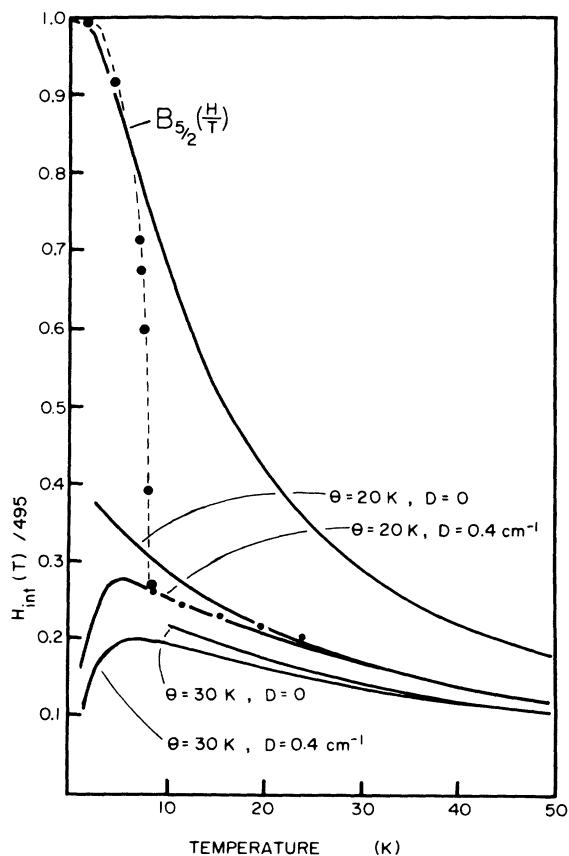


FIG. 3. Curves are calculated with different molecular field interactions θ and various zero-field splittings D . The experimental points (dots) indicate quite clearly that there is a significant effect due to antiferromagnetic exchange in the paramagnetic region. The dashed curve indicates the behavior of the hyperfine field below T_N .

$$3C_e = DS_z^2 + 2\mu_B \vec{H}_m \cdot \vec{S}, \quad (4)$$

where

$$H_{mA} = H_0 - N_1 M_A - N_2 M_B \quad (4a)$$

and

$$H_{mB} = H_0 - N_2 M_A - N_1 M_B; \quad (4b)$$

$$H_m = H_{mA} = H_{mB}$$

in the paramagnetic region.

H_{mA} is the total field sensed by the electronic moment on sublattice A, H_0 is the applied field, M_A and M_B are the sublattice magnetizations. This molecular field model would require for the internal field (assuming $D=0$)

$$H(T) = H(0) B_{5/2} \frac{H_m}{T} = H(0) B_{5/2} \left(\frac{H_0}{T + \Theta} \right),$$

where Θ is the paramagnetic Néel temperature given by $\Theta = \frac{1}{2} C(N_1 + N_2)$. This is clearly an improvement, as seen in Fig. 3, but still does not bring full agreement between the model and the experiment.

It is of some interest to note that the data lie within the regions where Θ is 20 and 30 K, in rough agreement with the $\Theta = 30.5$ K found by Jones *et al.*⁸ and $\Theta = 14$ K determined by Bizette *et al.*⁹

Better agreement is obtained by taking into account the zero-field splitting D . We expect the term DS_z^2 to be fairly small since $D = 0.189 \text{ cm}^{-1}$ for Fe^{3+} in isomorphous AlCl_3 ,¹⁷ but with $D = 0.4 \text{ cm}^{-1}$, together with $\Theta = 20$ K, fairly good agreement is obtained as shown in Fig. 3, which is as much agreement as can be expected from mean-field models. Nevertheless, this gives confidence in a general understanding of the model. It should be noted that the zero-field splitting D has the effect of depopulating the $m_s = \pm \frac{5}{2}$ states at low temperatures so that the effective hyperfine field will correspond to that of a spin less than $\frac{5}{2}$.

B. Antiferromagnetic Region—Zero Applied Field

The data in Fig. 4 were fit by a least-squares method to determine the hyperfine field at each temperature. The data below about 8.5 K are easily fit to six peak magnetic patterns even though the lines broaden as the critical region is approached. The Mössbauer patterns near the critical temperature show extreme broadening so that it is not such a simple matter to fit the data nor to interpret it. However, the temperature dependence of the hyperfine field is well represented by a power law of the form

$$H(T) = H(0) B(1 - T/T_N)^{\beta^*} \quad (5)$$

for almost all temperatures less than T_N , as shown in Fig. 5. The parameters B , T_N , and β^* were determined by a least-squares method and

the following values were obtained:

$$B = 1.035, T_N = 8.76 \text{ K}, \beta^* = 0.156.$$

The experimental value of H at $T=0$ is 495 kOe. There are several unusual aspects of the temperature dependence of the hyperfine field that should be remarked upon. The first is the unusually good

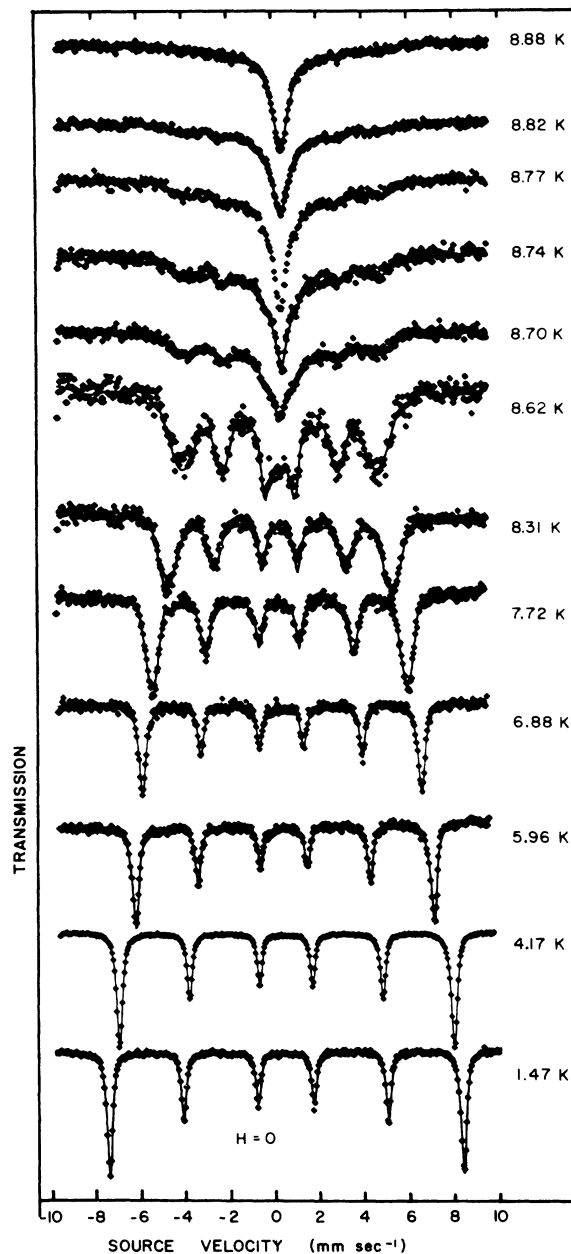


FIG. 4. Mössbauer data for FeCl_3 at several temperatures below the Néel temperature T_N in zero applied field. Notice the broadening in the resonance lines as the temperature approaches T_N , as well as the diminishing hyperfine field.

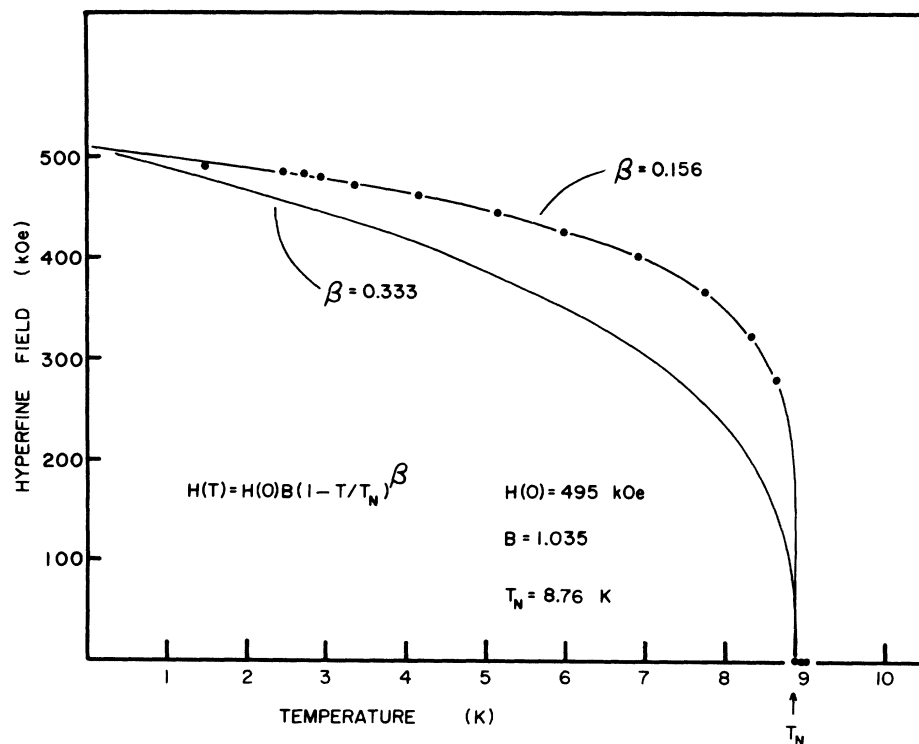


FIG. 5. Temperature dependence of the hyperfine field in FeCl_3 as determined by fitting the spectra in Fig. 4. The solid curve with $\beta = 0.156$ is fit to the data. The curve with $\beta = 0.333$ is shown for comparison.

fit for $H(T)$ for nearly all temperatures less than T_N . Usually, good agreement is found only in the region down to $\frac{1}{2}T_N$.

The saturation value for the hyperfine field at $T=0$ is unusually small for a ferric ion. This compares with the values found in some covalent materials¹⁸ and is much smaller than the "ionic" value of 620 kOe.¹⁹ Apparently, there are considerable covalency effects—delocalization of the magnetic electrons from the iron itself, but perhaps also negative contributions from neighboring spins. Zero point motion of the spins cannot account for such a large reduction.

Perhaps the most interesting result is the value of the exponent β^* . This parameter is quite sensitive²⁰ to the values chosen for T_N but has questionable meaning for temperatures not in the immediate vicinity of the critical temperature T_N . Nevertheless, the temperature dependence of the hyperfine field is quite well explained by the power law. We define β^* to be the slope of the curve $\ln(H)$ vs $\ln(1 - T/T_N)$ for all temperatures below T_N . Of course as $T \rightarrow T_N$ then $\beta^* \rightarrow \beta$, which is the true critical exponent. The determination of critical exponents has recently been a topic of much interest in the literature of magnetism. The molecular field theory predicts $\beta = \frac{1}{2}$, the three-dimensional Heisenberg model gives $\beta \approx \frac{1}{3}$ as calculated from several series expansions. Onsager's famous solution to the two-dimensional Ising model gives $\beta = \frac{1}{8} = 0.125$. The value of $\beta \approx 0.156$

determined from our experiments coupled with the layer-type structure in FeCl_3 initially gave rise to speculation that perhaps there is two-dimensional order in FeCl_3 . Such behavior has been observed³ in K_2NiF_4 , KMnF_4 , and RbFeF_4 , in which similar values of β were obtained from neutron data and, more importantly, two-dimensional correlations were observed. However, such a study²¹ has shown that FeCl_3 has only three-dimensional order below 12 K despite the low value of β^* .

Another possible explanation is that the small value of β^* could in fact be due to a first-order transition which occurs very near the T_N used in the power law and which is seen in neutron scattering results (0.07 K) below T_N . Our data show no evidence of this but the relaxation effects in the Mössbauer data near T_N would mask such behavior. It is not clear what the implications of a first-order transition are with regard to the temperature dependence of the hyperfine field for $T < T_N$.

As mentioned above, the Mössbauer resonance lines become extremely broad for temperatures just below the critical temperature but are quite narrow for the lower temperatures. These are several effects which could give rise to such a broadening of the lines. As we have seen, the temperature dependence of the hyperfine field is well represented by the power law of Eq. (4). If there were a distribution of temperatures in the sample there would then be a distribution of hyper-

fine fields. A small change in the temperature dT gives rise to a small change in the hyperfine field dH , where

$$dH = \beta H(0) B \left(1 - \frac{T}{T_N}\right)^{B-1} \left(\frac{-dT}{T_N}\right) \quad (6)$$

or

$$\frac{dH}{H} = -\beta \left(1 - \frac{T}{T_N}\right)^{-1} \frac{dT}{T_N} \quad (7)$$

Thus when $T \rightarrow T_N$ even a small deviation in temperature will give rise to a relatively large deviation in hyperfine field. The data of Fig. 4 were fit by assuming a Gaussian distribution of temperatures in the sample which causes the broadening. The width of this distribution was found to be 0.15 K. The sample was a single crystal and was entirely within an aluminum enclosure anchored to a copper sample holder. This provides an isothermal shield and there should be no distribution of temperatures in the sample once equilibrium is reached. Equilibrium would certainly be obtained in a few minutes while the data were taken for periods no less than 24 hours.

A second possibility might be instability in the temperature controller over the course of the experiment. An electrothermal feedback technique was used¹⁶ and the temperature monitored for each experiment on a chart recorder which indicated a constant temperature to better than 40 millidegrees for each experiment. Such a change in temperature over the course of an experiment is too small to account for the observed broadening.

A third possible explanation is the existence of a distribution of Néel temperatures in the single-crystal example. Stacking faults and slippage of the layers of FeCl_3 could give rise to this behavior. The data were fit assuming a Gaussian distribution of Néel temperatures. The change in hyperfine field due to a change in Néel temperatures is

$$\frac{dH}{H} = \beta \left(1 - \frac{T}{T_N}\right)^{-1} \frac{T dT_N}{T_N^2} \quad (8)$$

The average width of the Gaussian for this assumption was determined to be more than 0.27 K for the data in Fig. 4. The width of this distribution of Néel temperatures would be a constant of the sample and one would not expect it to be temperature dependent. This behavior has been discussed elsewhere.²²

Lastly, the possibility of relaxation effects becoming important near the critical temperature was investigated. The spectra are similar to those calculated according to a model developed by Wickman²³ in which the hyperfine field is allowed to fluctuate between two sublevels, but a detailed fitting according to this model was not possible.

After consideration of the above-mentioned possibilities it appears that the best explanations for

the broad lines just below T_N are the latter two. Of these two, the data accumulated in large magnetic fields show that the relaxation model is probably the correct one and we shall return to this point later.

The spins are in a spiral in zero magnetic field.⁴ Further neutron experiments by Endoh *et al.*²¹ on single crystals cut from the same boule as the Mössbauer absorbers have verified the spiral structure proposed by Cable *et al.*⁵ This model is consistent with the measured relative intensities of the six lines in zero field.

C. Antiferromagnetic Region in Applied Fields—Magnetic Phases

Mössbauer data were taken in the presence of magnetic fields up to 60 kOe applied along the c axis of the FeCl_3 crystals at temperatures up to 25 K.

The Mössbauer spectra in applied fields near T_N exhibit extremely broad lines as in the zero-field data so that there is some uncertainty in making a distinction between antiferromagnetic (A) and paramagnetic (P) phases. As discussed previously for the zero-field data, it appears that there are relaxation effects which cause the broadening near the critical temperature. Nevertheless, the temperature uncertainty in the boundary between the paramagnetic and antiferromagnetic states is less than 0.2 K. The A - P boundary was determined by taking Mössbauer spectra with the same value of the applied field and at different temperatures. Representative spectra are shown in Fig. 6.

As the applied field is increased at 4.2 K from zero to about 15 kOe one observes that the lines in the spectrum broaden, and that the hyperfine field decreases. The zero-field spin structure is helical with the axis of the helix in the $[1450]$ direction (normal to the c axis and the applied field) so that the magnetic spins make various angles with the applied field. As the field is increased, one would expect a further broadening of the Mössbauer lines owing to the vector addition of the applied field to the hyperfine fields which (in the spiral structure) are at various angles to the c axis (multiples of 12° from 0° to 360°).

A broadening of the six lines is observed, but for fields above 15 kOe (and below the spin-flop field of 40 kOe) it was found that a two-sublattice model gave better fits to the data than the spiral structure. This can be seen qualitatively in Fig. 7, where there are two distinct six-line spectra resolved in this regime. Thus the spiral appears to be destroyed somewhere below 15 kOe, where the resolution of the Mössbauer experiment was not sufficient to detect the change. It happens that both models give the same relative intensities for the Mössbauer resonances.

A considerable effort was put into least-squares

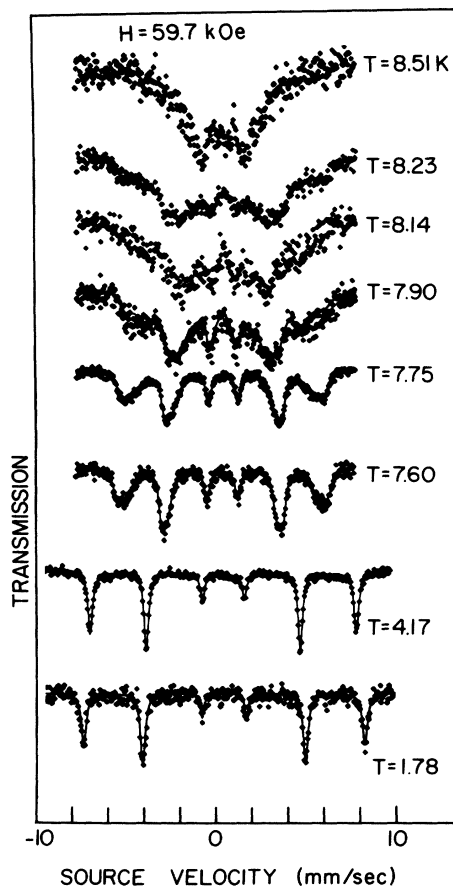


FIG. 6. Mössbauer spectra of single-crystal FeCl_3 in a field of 59.7 kOe applied in the c direction near the boundary between the paramagnetic and magnetically ordered regions. The lines are broad near the Néel temperature as with the zero-field spectra. Similar data were taken fields of 51, 40, and 30 kOe.

fitting the data where the two sets of six lines were observed. It needs to be emphasized that, with a single crystal of known orientation in an applied magnetic field and with a specific γ -ray direction, there is information in the spectra concerning the distributions of magnetization in both amplitude and direction. The spectra proved very difficult to fit and after some efforts based on various models suggested by the spiral arrangement, a more general fitting program was written. Here the distributions in angle and hyperfine field were represented by Fourier series, and the coefficients of the terms were determined by least-squares fitting of the data. It was found that the best fits to these data always gave two peaks in the hyperfine-field distributions and two peaks in the angular distribution near 54° and 126° from the c axis. This suggests a two-sublattice model, which was tried and indeed found to give the best

fits. The fits were still not entirely satisfactory, which we attribute to the broadening of the lines owing to sample thickness and in part to relaxation effects. The angles found were $54^\circ \pm 6^\circ$ and

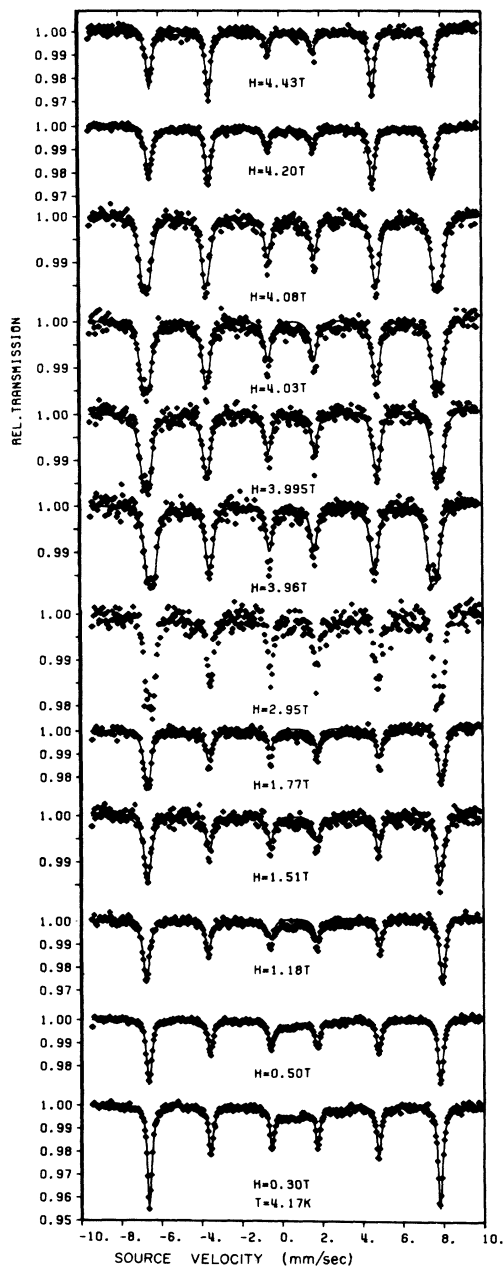


FIG. 7. Mössbauer spectra for FeCl_3 single crystals at 4.2 K with variable applied fields in the c direction. A reorientation of the spins is seen to take place at about 40 kOe. It is also seen that there are apparently two sublattices for fields just below the spin-flip field indicating the destruction of the spiral-spin configuration which exists in zero field. The applied field is indicated in mks units ($1\text{T} = 10\text{ kOe}$). Similar data were taken at 2.2, 5.3, 6.5, 7.8 K.

$126^\circ \pm 8^\circ$ relative to the c axis, showing that for fields of 15–40 kOe, the spins probably point at one of the chlorine near neighbors which are at $53^\circ 11'$ and $126^\circ 48'$ relative to the c axis.

For applied fields greater than 40 kOe there is an apparent reorientation of the electronic spins as indicated by the intensities of the $\Delta m = 0$ transitions (lines 2 and 5 of the six-line pattern) relative to the intensities of the inner lines (3 and 4). The ratio of these intensities changed from $\frac{1}{3}$ in the A phase to nearly $\frac{4}{1}$ in what we shall call the spin-flop (SF) phase. The changes in intensities with small changes in the applied fields (at constant T) are shown in Fig. 7. It was recently observed by Jaccarino *et al.*²⁴ that it is possible to get domain structures in spin-flop transitions; i. e., some regions have flopped onto the SF phase while others are still in the A phase. This effect will give the transition a finite width. The boundary between the A and SF phases has been measured at 2.2, 4.2, 5.3, 6.5, and 7.8 K (see Fig. 8) and it is seen that it increased from about 39 kOe at low temperature to about 49 kOe as extrapolated to the paramagnetic boundary, giving a triple point at

(8.4 K, 49 kOe).

The boundaries which separate the A , SF, and P phases of FeCl_3 in the H - T plane in Fig. 8 are determined with the field applied along the c axis. Ferric chloride is not a simple uniaxial antiferromagnet since it has a spiral-spin structure in zero applied fields. However, as mentioned above, there is evidence that the spins make only two angles relative to the c axis for fields up to the spin-flop field.

This would be consistent with a two-sublattice model but certainly does not preclude an arrangement in which the spins lie on cones making dihedral angles of 54° and 126° with the c axis in the presence of a field in the c direction. In either case the applied field in the c direction is not along the easy axis of the spins.

Nevertheless, a spin reorientation is observed when the applied field exceeds the spin-flop field. This reorientation seems to occur over a range of a few hundred oersted, as determined from our experiments. The molecular field theory²⁵ for a uniaxial antiferromagnet does not apply to the complicated spin structure of FeCl_3 , but we will use

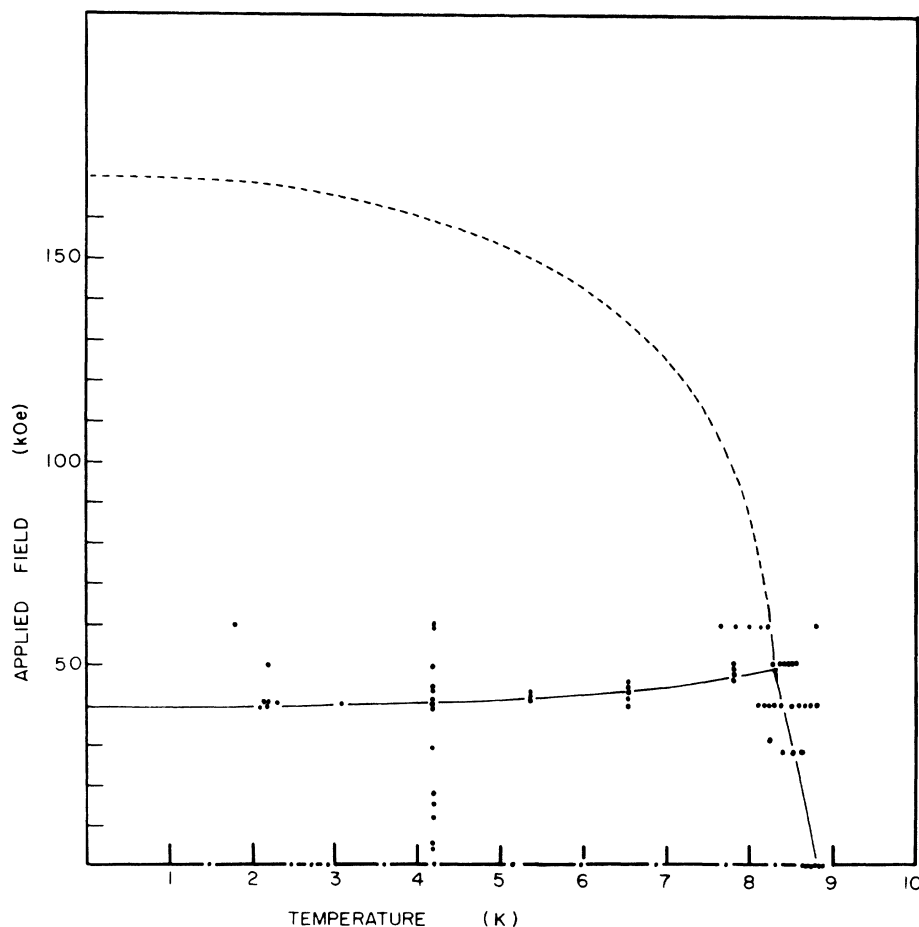


FIG. 8. Magnetic phase boundaries in the H - T plane determined from the experimental Mössbauer spectra. Each dot in the figure indicates one of the experimental Mössbauer spectra. The dashed curve is an estimate only.

its framework to describe the phenomena we have observed and to provide estimates for the regions in the H - T plane not accessible in our laboratory. The exchange field H_E can be related to the zero-field critical temperature T_N since they each depend upon the exchange interactions. If only z nearest neighbors with exchange interaction J are considered, then $H_E = 3kT_N/g\mu_B(S+1) = 56.3$ kOe.

However, experiments show that $T_N \neq \Theta$, which commonly occurs in antiferromagnets and is usually attributed to exchange interactions with different sublattices. In such cases, the paramagnetic Néel temperature Θ is usually a better estimate for the exchange field. For $\Theta = 14$ K⁹ we find $H_E = 3k\Theta/g\mu_B(S+1) = 89$ kOe. The spin-flop field H_f we have measured as 39 kOe at zero temperature and since

$$H_f = \left(\frac{2H_E H_A + H_A^2}{(1 - \chi_{||}/\chi_{\perp})} \right)^{1/2}$$

(with $\chi_{||} = 0$ at $T = 0$) we can solve for the anisotropy field $H_A = 8$ kOe. We can then estimate $H_c = 2H_E - H_A \approx 170$ kOe (see Fig. 8). This would appear to be a reasonable estimate and we will leave this number for other experimenters to measure.

There has been a recent discussion by Robinson and Erdos²⁶ which concerns the helical-spin structure with an applied field in the plane of the spins and perpendicular to the axis of the helix. This calculation coincides with many of the conditions for the experiments done on ferric chloride and some of the observed phase changes appear to be in qualitative agreement with the calculation.

IV. LINE BROADENING NEAR THE CRITICAL TEMPERATURE

It is seen both in the zero-field spectra (Fig. 4) and the spectra taken in applied fields (Fig. 6) that the resonance lines broaden as the critical temperature is approached. This behavior can be interpreted as due either to a distribution of Néel temperatures or to spin relaxation effects in the Mössbauer spectrum, or perhaps to both of these.

One might think that there are components in the spectrum which could be due to a part of the sample which is paramagnetic because of a smaller critical temperature while the rest of the sample remains magnetically ordered. However, if these are paramagnetic ions, then the induced hyperfine fields due to the applied field should be predicted by the theory discussed above for the paramagnetic region and should continue smoothly along the curve indicated by the experimental points. Clearly the data for temperatures below 8.5 K are not paramagnetic. The asymmetric shape of the lines in Fig. 6 is most likely due to a distribution in angle that the hyperfine fields make with the γ beam. In going from the paramagnetic to the flopped state

the electronic spins have to rotate from a direction parallel to the field, and γ rays to an orthogonal direction. The neutron-diffraction results of Endoh *et al.* give some support to the range of Néel-temperature hypothesis; they observed a possible first-order transition with hysteresis effects near T_N in which the slope of the magnetization is noninfinite.

Our favored explanation of this broadening is that as the critical temperature is approached fluctuations of the internal-field direction increase owing to spin relaxation, and in fact become comparable to the Larmor-precession rate of the nucleus. These broad spectral lines have been observed in a number of Mössbauer studies of high-spin ferric salts,^{27,28} and also in ferrous carbonate.²⁹ Two different mechanisms can account for the relaxation behavior of such systems, but it is difficult to distinguish between them on the basis of fitting the data because of the difficulty in treating the relaxation theoretically. A simple fit using a two-sublevel system is unsatisfactory on either model.

The first mechanism follows the theory of super antiferromagnetism³⁰ and postulates that as one approaches the Néel point, the anisotropy energy over a small region becomes comparable to the thermal energy, such that the magnetization vector fluctuates rapidly owing to the thermal excitation. Inside the region there is still antiferromagnetic order, but its direction is changing at a rate comparable to the Larmor-precession time of the nucleus. The second mechanism is based on a more fundamental property, namely, that of the critical slowing down of the spin fluctuations as the Néel point is approached (see the discussion by Walker, Munley, and Loh on ferrous carbonate).

At 8.23 K in Fig. 6 and in the zero-field data above 8.62 K in Fig. 4, the data indicate absorption in the wings of the spectrum which would be possible for a slowly relaxing spin system but not for the model with a distribution of Néel temperatures. This absorption in the wings moves toward smaller fields or stays constant as the temperature is lowered and the spin relaxation rate increases.

For the distribution-of-Néel-temperature hypothesis, there should be an increase in the average hyperfine field as the temperature is lowered. In any case, the results are inconclusive.

V. DISCUSSION

The data in the paramagnetic region (in applied fields) are fairly well understood when exchange interactions are taken into account. The paramagnetic Néel temperature found from this data ($\Theta \sim 20$ K) is in rough agreement with earlier susceptibility measurements. It was necessary to

taken into account the zero-field splitting ($D \sim 0.4 \text{ cm}^{-1}$) due to anisotropies in the local environment. However, the lack of a resolved quadrupole splitting indicating a nearly cubic environment would seem to be in conflict with this hypothesis. As noted in an earlier section, the spins make an angle of 54° with the c axis, which we take to be the anisotropy axis, and it is well known that for this particular angle between the spin direction and the principal axis of the field gradients there is no shift in the magnetically split lines due to the quadrupole interaction. This could explain the lack of an observable quadrupole interaction in the antiferromagnetic region, but would not explain the lack of such an interaction in the paramagnetic region, or the spin-flop region. Thus, we cannot explain the existence of a relatively large D , with the absence of any electric field gradient.

In a two-sublattice molecular field model, the paramagnetic Curie temperature Θ and the actual Néel temperature T_N are related to the exchange interactions of the two sublattices as given by Morrish³¹:

$$\Theta = \frac{1}{2} C(N_1 + N_2) \geq 14.0 \text{ K}$$

(we take Bizette's value⁹ as a lower limit),

$$T_N = \frac{1}{2} C(N_2 - N_1) = 8.76 \text{ K.}$$

From these it is found that $N_1 = 5.2C$ and $N_2 = 22.8C$, where C is the Curie constant.

We note that the ratio of the exchange between the two sublattices (N_2) to the exchange within a sublattice (N_1) is $N_2/N_1 = 22.8/5.1$ or greater if larger values for Θ are used. Pairs of spins in the c direction are antiferromagnetically aligned while the spins in the plane perpendicular to c have three equivalent near-neighbor interactions. We will take the ferric ions in alternate layers perpendicular to the c axis as one sublattice with the other sublattice sandwiched in between. There are at least three near neighbors in the plane while the one near neighbor in the c direction is antiparallel. In terms of the molecular field model the interaction between sublattices $z_2 J_2$ is due to only one near neighbor ($z_2 = 1$), while the interactions within the layer are due to three or more neighbors ($z_1 = 3$). Thus the ratio of exchange between sublattices to the exchange within a sublattice is at least $z_2 J_2 / z_1 J_1 = J_2 / 3J_1 = 22.8/5.2$ or $J_2 / J_1 = 13.1$. This is fairly anisotropic and reflects the strength of the interaction in the c direction compared to the interactions within the plane. The existence of a spiral-spin structure in the plane is itself evidence for delicately balanced interactions among several sets of neighbors in the plane, so that N_1 probably has more than 3 contributions.

As mentioned above, there is considerable line broadening in the region near the critical tempera-

ture which is attributed to relaxation effects. Recent neutron scattering experiments²¹ indicate a first-order transition in zero applied field which is not evident from the Mössbauer results. However, both neutron and Mössbauer-effect studies determine an exponent $\beta^* \sim 0.156$ which is reduced from the usual three-dimensional value of $\beta = 0.333$. It is also noteworthy that the measured T_N differs in the two experiments by a significant amount. The samples for the two experiments were cut from the same crystal. Since it has been established²⁰ that the exponent β^* is quite dependent on the value chosen for T_N , it is remarkable how the same β^* was found from the two experiments for which T_N differs by about 10%. This would be possible if there were simply a constant factor between thermometers since β^* is simply the slope of $\ln H$ vs $\ln(1 - T/T_N)$. It is also possible that the different times of measurement inherent in the different techniques can influence the result for T_N .³²

The small value of β^* is apparently not due to two-dimensional ordering in view of the lack of two-dimensional correlations in the neutron experiments. However, recent calculations by Bonner and Nagle^{33,34} have shown the reduction of β^* from 0.50 to 0.25 when the system is in the vicinity of a hypercritical point for a molecular field model with competing interactions. We note that we seem

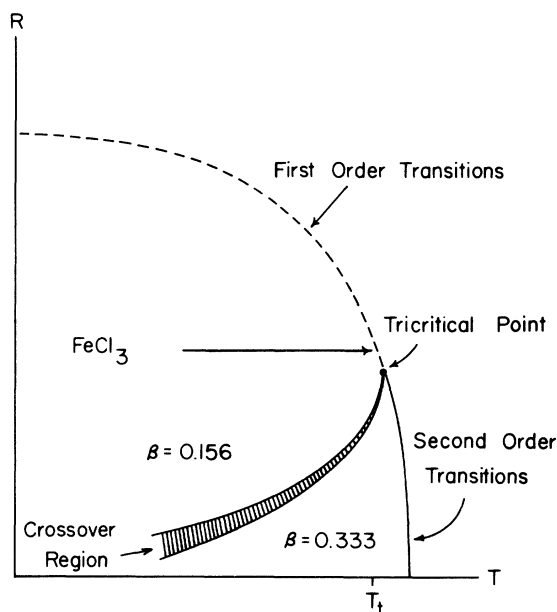


FIG. 9. Diagram indicating the tricritical point at which the line of second-order transitions and a line of first-order transitions meet. The parameter R has to do with the ratio competing exchange interactions and is a variable which cannot be controlled in the laboratory. The other coordinate is the temperature of the sample.

to have a reduction in β from 0.33 to 0.16, also a factor of 2.

If the physical conditions are such that the system is precisely at a hypercritical point then the exponent β^* will have a reduced value for all temperatures through the critical temperature. However, if one is merely *near* a hypercritical point, then for temperatures below the critical region one would observe a reduced value of β^* , but as the critical region is approached, there is a crossover where $\beta^* \rightarrow \beta$ and it takes on its usual three-dimensional value. Since only three-dimensional correlations have been observed in the neutron scattering experiments, this explanation for the reduced value of the exponent appears to fit the available data.

In the neutron experiments, there is some evidence for a first-order transition only 70 millidegrees below the critical temperature found by extrapolation of the power law. The existence of a nearby hypercritical point is consistent with this first-order transition (see Fig. 9), and with the fluctuations observed near the ordering temperature. Also the fact that FeCl_3 exhibits a spiral-

spin structure in zero applied field is good evidence for competing interactions.

Other techniques show some of the same exponents³⁵ but no other evidence for a tricritical point.³⁶ It may be that there are different crossover regions for different critical exponents.

The magnetic phase boundaries have been determined roughly in fields up to 60 kOe applied in the *c* direction. Hopefully, more accurate determinations of these boundaries can be made by other techniques. Further study with Mössbauer spectroscopy would be costly and not lead to significant improvement in the accuracy of these phase boundaries. It would also be of interest to learn the precise behavior of the relaxation of the hyperfine field near T_N , which appears to give such difficulty in the Mössbauer data of FeCl_3 .

ACKNOWLEDGMENTS

It is a pleasure to acknowledge several helpful discussions with Professor S. A. Friedberg, Professor J. F. Nagle and Professor J. C. Bonner, Professor P. Flinn and Dr. G. Shirane, Dr. J. Skalyo, and Dr. Y. Endoh.

[†]Work supported in part by the National Science Foundation and by the Office of Naval Research.

*Present address: Bell Telephone Laboratory, Holmdel, N. J. 07733.

[‡]Present address: Solid State Physics Dept., Australian National University, Canberra, A. C. T., Australia 2600.

¹N. Wooster, *Z. Kristallogr.* **83**, 85 (1932).

²S. Blairs and R. A. J. Shelton, *J. Inorg. Nucl. Chem.* **28**, 1855 (1966).

³R. J. Birgeneau, H. J. Guggenheim, and G. Shirane, *Phys. Rev. B* **5**, 2211 (1970); J. Skalyo, Jr., G. Shirane, and S. A. Friedberg, *Phys. Rev.* **188**, 1037 (1969).

⁴C. Starr, F. Bitter, and A. R. Kaufmann, *Phys. Rev.* **58**, 977 (1940).

⁵J. W. Cable, M. K. Wilkinson, E. O. Wollan, and W. C. Koehler, *Phys. Rev.* **127**, 714 (1962).

⁶C. W. Kocher, *Phys. Lett. A* **24**, 93 (1967).

⁷E. Pfletschinger, *Z. Phys.* **209**, 119 (1968).

⁸E. R. Jones, Jr., O. B. Morton, L. Cathey, T. Auel, and E. L. Amma, *J. Chem. Phys.* **50**, 4755 (1969).

⁹H. Bizette, A. Adam, and N. Ciret, *C.R. Acad. Sci. (Paris)* **271**, 608 (1970).

¹⁰J. W. Cable, M. K. Wilkinson, E. O. Wollan, and W. C. Koehler, *Phys. Rev.* **125**, 1860 (1962).

¹¹T. Moriya and T. Nagamiya (private communication).

¹²H. Schafer and L. Bayer, *Z. Anorg. Allg. Chem.* **272**, 18 (1953).

¹³R. W. Bene, *Phys. Rev.* **178**, 497 (1969).

¹⁴R. C. Weast, *Handbook of Chemistry and Physics*, 51st ed. (Chemical Rubber Co. Cleveland, 1971).

¹⁵C. E. Violet and D. N. Pipkorn, University of California Radiation Laboratory Report, 1970 (unpublished).

¹⁶B. Window, *J. Phys. E* **2**, 894 (1969).

¹⁷G. Bang, G. Sperlich, and W. J. Becker, *Phys. Status Solidi* **41**, 369 (1970).

¹⁸G. Lang, *Q. Rev. Biophys.* **3**, 1 (1970).

¹⁹R. E. Watson and A. J. Freeman, *Phys. Rev.* **123**, 2027 (1963).

²⁰P. Heller, *Phys. Rev.* **146**, 403 (1966); G. K. Wertheim, *Phys. Rev.* **169**, 465 (1968).

²¹Y. Endoh, J. Skalyo, W. T. Oosterhuis, and J. Stampfel, *AIP Conf. Proc.* **10**, 98 (1973).

²²D. E. Earls, R. C. Axtmann, and Y. Hazony, *J. Phys. Chem. Solids* **29**, 1859 (1968).

²³H. H. Wickman, in *Mössbauer Effect Methodology*, edited by I. J. Gruverman (Plenum, New York, 1966), Vol. 2, p. 39.

²⁴V. Jaccarino, *Perspectives for Hyperfine Interactions in Magnetically Ordered Systems by NMR and Other Methods* (L'Aquila, Italy, 1972).

²⁵F. Keffer, *Handbuch der Physik*, edited by H. P. J. Wijn (Springer-Verlag, Berlin, 1966), Vol. XVIII 2, p. 1.

²⁶J. M. Robinson and P. Erdos, *Phys. Rev. B* **2**, 2642 (1970).

²⁷F. Van der Woude and A. J. Dekker, *Phys. Status Solidi* **13**, 181 (1966).

²⁸L. Levinson, M. Luban, and S. Shtrikman, *Phys. Rev.* **117**, 864 (1969).

²⁹J. C. Walker, F. Munley, and E. Loh, in *Proceedings of the Conference on Applications of the Mössbauer Effect, Tihany, 1969*, edited by I. Dezi (Akademiai Kiado, Budapest, 1971), p. 153; H. N. Ok, *Phys. Rev.* **185**, 472 (1969).

³⁰L. Néel, *J. Phys. Soc. Jap. Suppl.* **17**, 676 (1962).

³¹A. H. Morrish, *The Physical Principles of Magnetism* (Wiley, New York, 1965) p. 447.

³²P. K. Iyengar and S. C. Bhargava, *Phys. Status Solidi B* **46**, 117 (1971).

³³J. C. Bonner and J. F. Nagle, *J. Appl. Phys.* **42**, 1280 (1971)

³⁴J. F. Nagle and J. C. Bonner, *J. Chem. Phys.* **54**, 729 (1971).

³⁵R. J. Birgeneau, J. Skalyo, and G. Shirane, *Phys. Rev. B* **3**, 1736 (1971).

³⁶R. B. Griffiths, *Phys. Rev. B* **7**, 545 (1973).